Fabrication and Characterization of Silver−Polyvinyl Alcohol Nanocomposites

Z. H. Mbhele,[†] M. G. Salemane,[†] C. G. C. E. van Sittert,[‡] J. M. Nedeljković,[§] V. Djoković,[†,§] and A. S. Luyt*[,†]

Department of Chemistry, University of the Free State (Qwa-Qwa), Private Bag X13, Phuthaditjhaba, 9866, South Africa, School of Chemistry and Biochemistry, Potchefstroom University, Private Bag 6001, Potchefstroom, 2520, South Africa, and Vinča Institute of Nuclear Sciences, P.O. Box 522, 11001 Belgrade, Serbia and Montenegro

Received June 18, 2003. Revised Manuscript Received October 17, 2003

The influence of silver (Ag) nanoparticles on the properties of poly(vinyl alcohol) (PVA) was investigated. The nanocomposite was prepared by mixing a colloidal solution consisting of silver nanoparticles with a water solution of PVA in appropriate ratios. Composite films with different contents of inorganic phase were obtained after solvent evaporation. The contents of the inorganic phase in the nanocomposites were determined by using atomic absorption spectroscopy (AA) for silver, and were found to be 0.19, 0.33, and 0.73 wt %. Transmission electron microscopy (TEM) of the nanocomposite films revealed the presence of Ag particles with average diameter of 20 nm. Comparison of the thermal properties of the pure polymer and the nanocomposite films showed that the thermal stability is improved by about 40 °C, and the glass transition temperature is shifted to a higher temperature up to 20 °C for the highest content of the nanofiller. An increase in Young's modulus and strength of the nanocomposite was also observed with an increase in Ag content, indicating significant reinforcement of the matrix in the presence of nanoparticles. Stress relaxation measurements revealed reduced stability of the nanocomposite upon prolonged loading, compared to the pure PVA matrix.

Introduction

Recently, polymer nanocomposites are the subject of increased interest because of the unique properties that can be achieved with these materials. Polymers are considered as a good host material for metal[1−15] and semiconductor[16−26] nanoparticles, which, on the other hand, exhibit exceptional optical and electrical properties. At the same time, because of their high surface-to-bulk ratio, nanoparticles significantly affect the matrix leading to some new properties which are not present in either of the pure materials. Therefore, the investigation of the influence of nanoparticles on the properties of a polymer matrix is necessary in order to be able to better predict the final properties of the composite.

Previous studies concerning the usage of noble-metal nanoparticles (Ag and Au) as a filler[1−10] are mostly concentrated on the structure and optical properties of the nanoparticles embedded in different matrixes. In these studies it was shown that optical properties of

* To whom correspondence should be addressed. Phone: +27-58-718-5306. Fax: +27-58-713-0152. E-mail: luytas@qwa.uovs.ac.za.
† University of the Free State.
‡ Potchefstroom University.
§ Vinča Institute of Nuclear Sciences.

(1) Zhu, Y.; Qian, Y.; Li, X.; Zhang, M. *Chem. Commun.* **1997**, 1081.
(2) Dirix, Y.; Bastiaansen, C.; Caseri, W.; Smith, P. *J. Mater. Sci.* **1999**, *34*, 3859.
(3) Akamatsu, K.; Takei, S.; Mizuhata, M.; Kajinami, A.; Deki, S.; Takeoka, S.; Fujii, M.; Hayashi, S.; Yamamoto, K. *Thin Solid Films* **2000**, *359*, 55.
(4) Zeng, R.; Rong, M. Z.; Zhang, M. Q.; Liang, H. C.; Zeng H. M. *Appl. Surf. Sci.* **2002**, *187*, 239.
(5) Zhu, Y.; Qian, Y.; Li, X.; Zhang, M. *Nanostruct. Mater.* **1998**, *10*, 673.
(6) Wenming, C.; Yuan, Y.; Yan, L. *Mater. Res. Bull.* **2000**, *35*, 807.
(7) Zhang, Z.; Han, M. *J. Mater. Chem. Commun.* **2003**, *13*, 641.
(8) Ung, T.; Liz-Marzán, L. M.; Mulvaney, P. *J. Phys. Chem. B* **2001**, *105*, 3441.
(9) Hussain, I.; Brust, M.; Papworth, A. J.; Cooper A. I. *Langmuir* **2003**, *19*, 4831.
(10) Cole, D. H.; Shull, K. R.; Baldo, P.; Rehn, L. *Macromolecules* **1999**, *32*, 771.
(11) Liu, H.; Ge, X.; Zhu, Y.; Xu, X.; Zhang, Z.; Zhang, M. *Mater. Lett.* **2000**, *46*, 205.
(12) Zavyalov, S. A.; Pivkina, A. N.; Schoonman, J. *Solid State Ionics* **2002**, *147*, 415.
(13) Wizel, S.; Margel, S.; Gedanken, A. *Polym. Int.* **2000**, *49*, 445.
(14) Wizel, S.; Margel, S.; Gedanken, A.; Rojas, T. C.; Fernández, A.; Prozorov, R. *J. Mater. Res.* **1999**, *14*, 3913.
(15) Nakao, Y. *J. Chem. Soc. Chem. Commun.* **1993**, *10*, 826.
(16) Godovsky, D. Y. *Adv. Polym. Sci.* **2000**, *153*, 165.
(17) Qian, X. F.; Yin, J.; Huang, J. C.; Yang, Y. F.; Guo, X. X.; Zhu, Z. K. *Mater. Chem. Phys.* **2001**, *68*, 95.
(18) Kumar, R. V.; Elgamiel, R.; Diamant, Y.; Gedanken, A. *Langmuir* **2001**, *17*, 1406.
(19) Kumar, R. V.; Palchik, O.; Koltypin, Y.; Diamant, Y.; Gedanken, A. *Ultrason. Sonochem.* **2002**, *9*, 65.
(20) Šajinović, D.; Šaponjić, Z. V.; Cvjetićanin, N.; Marinović-Cincović, M.; Nedeljković, J. M. *Chem. Phys. Lett.* **2000**, *329*, 168.
(21) Yu, S.-H.; Yoshimura, M.; Moreno, J. M. C.; Fujiwara, T.; Fujino, T.; Teranishi, R. *Langmuir* **2001**, *17*, 1700.
(22) Djoković V.; Nedeljković, J. M. *Macromol. Rapid Commun.* **2000**, *21*, 994.
(23) Qiao, Z.; Xie, Y.; Chen, M.; Xu, Y.; Zhu, Y.; Qian, Y. *Chem. Phys. Lett.* **2000**, *321*, 504.
(24) Qiao, Z.; Xie, Y.; Zhu, Y.; Qian, Y. *J. Mater. Chem.* **1999**, *9*, 1001.
(25) Wang, Y.; Suna, A.; Mahler, W.; Kasowski, R. *J. Chem. Phys.* **1987**, *87*, 7315.
(26) Kumar, R. V.; Koltypin, Y.; Cohen, Y. S.; Aurbach, D.; Palchik, O.; Felner, I.; Gedanken, A. *J. Mater. Chem.* **2000**, *10*, 1125.

10.1021/cm034505a CCC: $25.00
Published on Web 11/22/2003

nanocomposites depend on the size and shape of particles, as well as on the type of polymer and/or the geometry of the samples (thin films, oriented films, or bulk samples). Poly(vinyl alcohol) (PVA) is a water-soluble polymer extensively investigated as a host for different kinds of nanofillers.[16−18,26−29] These investigations suggest that the introduction of nanosized particles into PVA alter its properties. However, different fillers affect the PVA matrix in different ways. For example, magnetite nanoparticles synthesized by a sonochemical method[26] reduce the glass transition temperature of PVA by 15 °C and the thermal stability by 28 °C, whereas in the presence of montmorillonite (MMT) nanofiller glass transition increases by 25 °C and the thermal degradation was unaffected up to 50% of initial weight loss.[27] In the latter study, PVA−MMT nanocomposites obtained by solution-casting from a water suspension also showed significant improvement of mechanical properties and reduced water-vapor permeability. In the present investigation, PVA−Ag nanocomposites were prepared by a similar procedure from water colloids consisting of Ag nanoparticles and the appropriate amount of PVA. Besides optical and structural properties of the nanocomposites, we focused on the thermal, mechanical, and viscoelastic behavior of PVA in the presence of low contents of Ag nanofiller (<1 wt %).

Experimental Section

Preparation of PVA−Ag Nanocomposites. Silver colloids were prepared by the reduction of silver ions using $NaBH_4$, as described elsewhere.[30] Briefly, a 10-mg sample of $NaBH_4$ was added to 100 mL of a vigorously stirred Ar-saturated solution of 5×10^{-5} M Ag_2SO_4. A clear yellow sol resulted. The pH increased due to the hydrolysis of excess $NaBH_4$ and after several minutes reached a value of 9.8. The described procedure leads to the formation of Ag particles with average diameter of 5 nm.

To prepare the PVA−Ag nanocomposite, the Ag colloid was combined in an appropriate ratio with PVA (BDH chemicals, $M_w = 140\,000$ g mol^{-1}, degree of hydrolysis 98%) dissolved in water. Finally, after evaporation of the solvent, yellow transparent PVA−Ag nanocomposite films were obtained. The films were dried at room temperature in air for 72 h. Their average thickness was about 400 μm. Pure PVA samples were prepared in the same manner.

Characterization of PVA−Ag Nanocomposites. The content of the inorganic phase in the nanocomposites was determined by atomic absorption analysis (Varian AA-1475) for Ag. Contents of Ag in the PVA−Ag nanocomposites were found to be 0.19, 0.33, and 0.73 wt % respectively.

Absorption spectra of Ag colloids in water, as well as the PVA−Ag nanocomposite films, were measured in the wavelength range from 300 to 700 nm using a Unicam UV−Vis spectrophotometer. FTIR spectroscopic analyses were carried out using a Nicolet Impact 410 FTIR spectrophotometer connected to a photoacoustic cell in the spectral range from 4000 to 400 cm^{-1}.

For transmission electron microscopy (TEM) measurements, the PVA−Ag nanocomposite samples were embedded in the resin and microtomed into electron beam transparent films using a Reichert-Jung Ultracut. TEM measurements were performed using a Phillps CM10 transmission electron microscope at 100 kV.

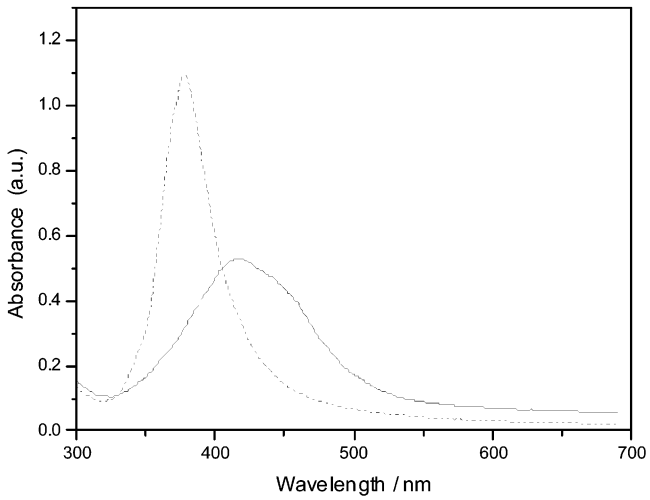

Figure 1. Absorption spectra of as-prepared silver colloid (dashed line) in water and PVA−Ag nanocomposite film (solid line) with 0.33 wt % of Ag.

Differential scanning calorimetry (DSC) measurements of the pure PVA and the PVA−Ag nanocomposites were performed using a Perkin-Elmer DSC 7 instrument in the temperature range from 25 to 250 °C under a nitrogen atmosphere. The heating and cooling rates were 20 °C min^{-1}. The thermogravimetric analyses (Perkin-Elmer TGA 7) of the pure PVA and the PVA−Ag nanocomposites with different content of inorganic phase were carried out in the temperature range from 50 to 600 °C under nitrogen atmosphere. The heating rate was 10 °C min^{-1}.

Mechanical and stress relaxation measurements were carried out using a Hounsfield H5KS tensile tester at a strain rate of 50 mm min^{-1}. Specimens were dumbbell shaped with 25-mm gauge length and 5-mm width. In the stress relaxation tests, samples were stretched to 2% strain and held in that position for 90 min. The relaxation of the stress was continuously monitored.

Results and Discussion

Optical and Structural Characterization of the PVA−Ag Nanocomposites. The absorption spectra of the colloidal solution containing Ag nanoparticles and the corresponding PVA−Ag nanocomposite film are shown in Figure 1. It can be seen that the surface plasmon absorption band of the initial water colloid is sharp, peaking at 380 nm. This result indicates narrow size distribution of the Ag nanoparticles with average diameter of 5 nm, and it is in agreement with our previous results.[30] On the other hand, the PVA−Ag nanocomposite film exhibits a broad surface plasmon absorption band peaking at approximately 420 nm. This result is in agreement with the optical absorption spectra of Ag nanoparticles embedded in different polymer matrixes: polyethylene,[2] nylon 11,[3] polystyrene, styrene-*co*-acrylonitrile,[4] and polyacrylonitrile.[7] The shift to the longer wavelengths and broadening of the surface plasmon absorption band upon incorporation of Ag nanoparticles into PVA can be induced by agglomeration of the Ag nanoparticles and/or change of the dielectric properties of the surrounding environment.

A typical TEM image of the PVA−Ag nanocomposite film is shown in Figure 2. The presence of spherical Ag particles with an average diameter of about 20 nm can be seen. This observation, supported by changes in the absorption spectra, indicates that agglomeration of the

(27) Strawhecker, K. E.; Manias, E. *Chem. Mater.* **2000**, *12*, 2943.
(28) Yu, Y.-H.; Lin, C.-Y.; Yeh, J.-M.; Lin, W.-H. *Polymer* **2003**, *44*, 3553.
(29) Schaffer, M. S. P.; Windle, A. H. *Adv. Mater.* **1999**, *11*, 937.
(30) Vuković, V. V.; Nedeljković, J. M. *Langmuir* **1993**, *9*, 980.

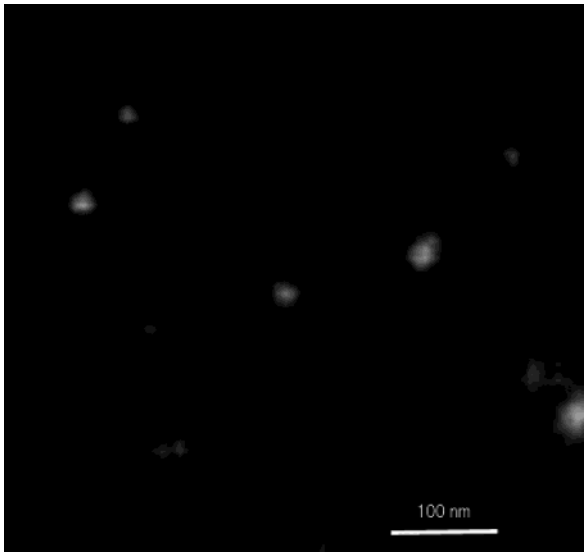

Figure 2. Transmission electron microscopy (TEM) micrograph of the PVA−Ag nanocomposite film (0.73 wt % of Ag).

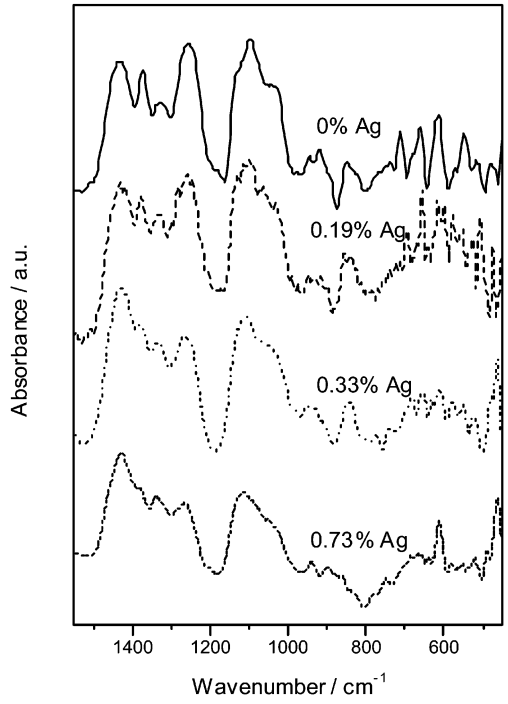

Figure 3. FTIR spectra of pure PVA and PVA−Ag nanocomposite films with different Ag contents (0.19, 0.33, and 0.73 wt %). For clarity the spectra are shown in the range from 450 to 1550 cm^{-1}.

Ag particles takes place during their incorporation into the polymer matrix. Despite the observed agglomeration our films maintain optical clarity.

To determine if chemical bonding between the PVA matrix and the Ag-nanofiller takes place, FTIR measurements of the pure PVA and the PVA−Ag nanocomposites with different content of inorganic phase were performed (see Figure 3). An increase in the Ag-nanofiller content leads to the disappearance of several bands (837, 711, 650, and 570 cm^{-1}). Bands at 570, 650, and 711 cm^{-1} are assigned to out-of-plane vibration of the O−H group, while the band at 837 cm^{-1} corresponds to the out-of-plane vibration of the C−H group. It should be emphasized that the band attributed to the out-of-plane O−H vibrations in alcohols is quite broad, from 550 to 750 cm^{-1}.[31] In our experiments, the photoacoustic cell is sufficiently sensitive to distinguish between specific peaks in this broad absorption range. The observed splitting is most likely a consequence of different surroundings of O−H group in the polymer matrix. It is important to point out that the disappearance of these bands suggests that interaction between Ag nanoparticles and the matrix takes place over the O−H groups. It also seems that attachment of the Ag nanoparticles to the PVA chains prevents the out-of-plane oscillations of the C−H group.

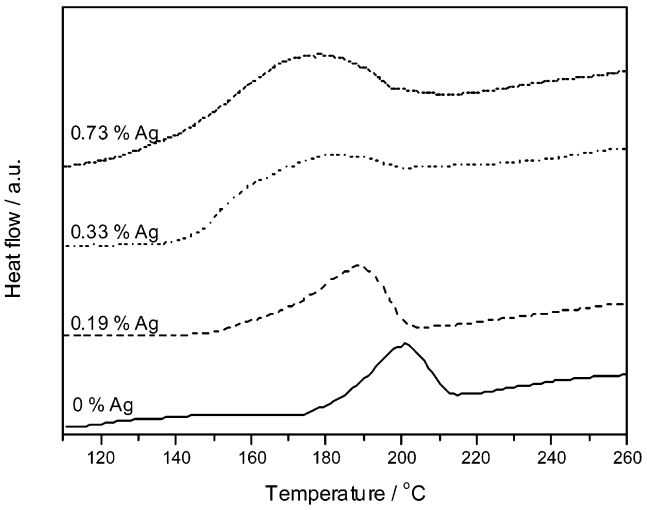

Figure 4. DSC curves of pure PVA and PVA−Ag nanocomposites with varying wt % of silver. For clarity, curves are presented in the range from 110 to 250 °C. (Heating rate 20 °C min^{-1}).

Another change in the IR spectrum of the PVA−Ag nanocomposite was observed for the band peaking at 1322 cm^{-1} (see Figure 3). In alcohols, this band is the result of the coupling of the O−H in-plane vibrations (strong line at 1420 cm^{-1}) with the C−H wagging vibration. Therefore, the decrease in the ratio between the intensities of this band and the band at 1420 cm^{-1} with an increase in the content of the inorganic phase indicates decoupling between the corresponding vibrations due to interaction between the Ag nanoparticles and the O−H groups originating from the PVA chains.

Thermal Characterization of the PVA−Ag Nanocomposites. The DSC heating curves of the pure PVA and the PVA−Ag nanocomposites are divided in two temperature regions (from 110 to 260 °C and from 60 to 130 °C) as shown in Figures 4 and 5, respectively. A summary of the DSC data which corresponds to these curves is shown in Table 1. The broadening of the melting peak, and its shift to lower temperatures with an increase in the inorganic phase content, can be seen in Figure 4. Although an increase in the nanoparticle content does not affect crystallinity (melting enthalpies in Table 1 are almost unchanged), it can be concluded that the presence of the Ag-nanofiller prevents crystal thickening. The observed effects can be explained by the reduced mobility of the PVA chains attached to the surface of the Ag nanoparticles. This is supported by the FTIR data.

(31) Silverstein, R. M.; Webster F. X. *Spectrometric Identification of Organic Compounds*; Wiley: New York, 1998; pp 85−90.

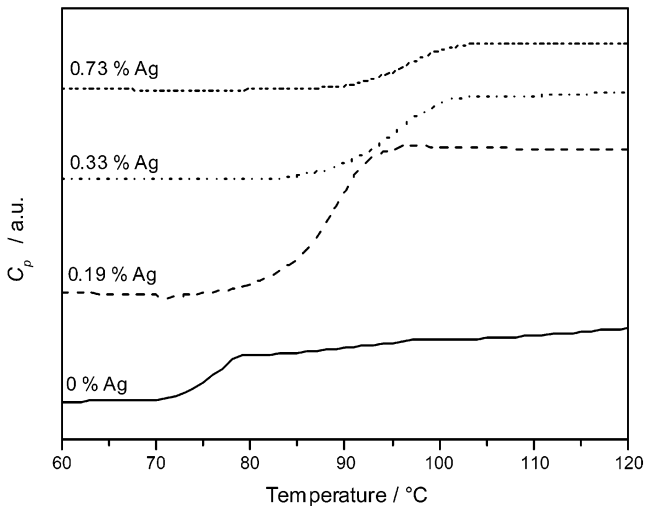

Figure 5. DSC heat capacity curves of PVA and PVA−Ag nanocomposites with varying wt % of silver. For clarity, curves are presented in the range from 60 to 130 °C. (Heating rate 20 °C min^{-1}).

Table 1. Melting Enthalpy (ΔH_m), Melting Peak Temperature (T_m), and Glass Transition Temperatures (T_g) of PVA and PVA/Ag Nanocomposites

wt % Ag	ΔH_m/J g^{-1}	T_m/°C	T_g/°C
0	17.9	200.4	76.1
0.19	19.7	190.0	87.8
0.33	18.1	161.7	94.9
0.73	21.1	177.7	97.0

The dramatic increase in the glass transition temperature by more than 20 °C for the nanocomposite with only 0.73 wt % of inorganic phase (see Figure 5 and Table 1), can also be explained by the reduced mobility of polymer chains. The glass transition, strictly speaking, is not a true phase transition, because the first derivative of the heat capacity curve is a continuous function of temperature as shown by phase-modulated DSC measurements. This implies that the polymer exhibits a spectrum of glass transition temperatures, each corresponding to different segmental relaxations. A close look at Figure 5 reveals not just a shift of the slope in the heat capacity curve to higher temperatures with an increase of the content of the inorganic phase, but also a broadening of its temperature range. It seems that incorporation of nanoparticles into the polymer matrix affects the distribution of chain segments, most likely due to a change in chain packing density in the vicinity of the surface of the nanofillers. It should be emphasized that strong effects, at such a low concentration of nanoparticles, on the matrix chains are unusual, since TEM shows that the distance between the particles is about 5 times the particle diameter. However, results of Zheng et al.[32] on polymer melt diffusion near an attractive surface could support our observations. They have observed long-range effects on polymer dynamics with an order of magnitude reduced diffusion rate relative to the bulk polymer, even at a distance 10 times the radius of gyration. Similar effects on the polymer melt show gold nanoparticles,[10] which increase the viscosity by a factor of 4. It seems that in this case silver particles affect the matrix further from the particle surface and/or partially prevent cooperative motions necessary for the glass transition to take place. Further investigations are in progress to clarify this behavior.

(32) Zheng, X.; Rafailovich, M. H.; Sokolov, J.; Strzhemechny, Y.; Schwarz, S. A.; Sauer, B. B.; Rubinstain, M. *Phys. Rev. Lett.* **1997**, *79*, 241.

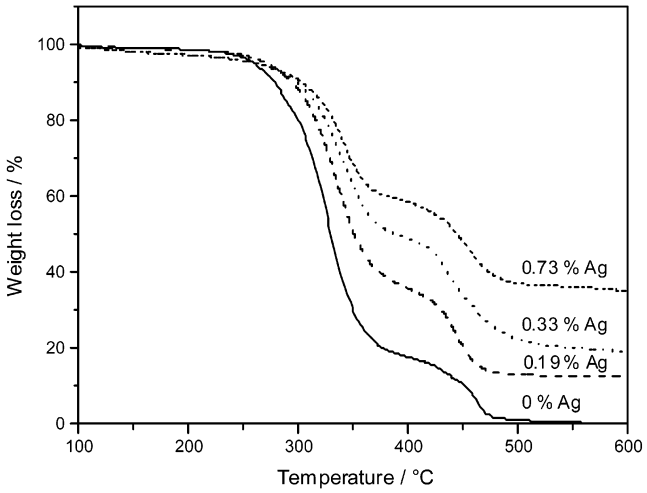

Figure 6. TGA curves of neat PVA and PVA−Ag nanocomposites obtained under nitrogen atmosphere and at a heating rate of 10 °C min^{-1}.

The observed DSC results differ from some results reported in the literature. For example, incorporation of magnetite particles, with average diameters of 12 and 20 nm, in the PVA matrix leads to a decrease in the glass transition temperature.[26] On the other hand, as in our case, glass transition increases after introduction of small amounts of montmorillonite (up to 5%) into PVA.[27] However, at montmorillonite contents higher than 4 wt %, the appearance of a new melting peak at higher temperatures was observed, while at the same time the decrease in intensity of the main PVA melting peak takes place.

The TGA measurements of the pure PVA and the PVA−Ag nanocomposites with different Ag contents are shown in Figure 6. An improvement in the thermal stability of the nanocomposite can be seen with an increase in the nanofiller content. For example, the onset of the thermal degradation is shifted to higher temperatures by about 40 °C for the composite with 0.73 wt % of Ag-nanoparticles. The degradation of polymers starts with free radical formations at weak bonds and/or chain ends, followed by their transfer to adjacent chains via interchain reactions. The improved thermal stability can be explained through the reduced mobility of the PVA chains in the nanocomposite. Because of reduced chain mobility, the chain transfer reaction will be suppressed, and consequently the degradation process will be slowed and decomposition will take place at higher temperatures. It is important to point out that the residual weight of the nanocomposite is more than one order of magnitude larger than the content of the inorganic phase at 600 °C, while at the same temperature the pure PVA is completely decomposed. This result indicates that the thermal decomposition routes of the pure PVA and the PVA−Ag nanocomposites are different. We believe that the observed behavior is most likely the consequence of the attachment of the PVA chains to the surface of the Ag-nanofiller. These results are in agreement with the thermal decomposition data

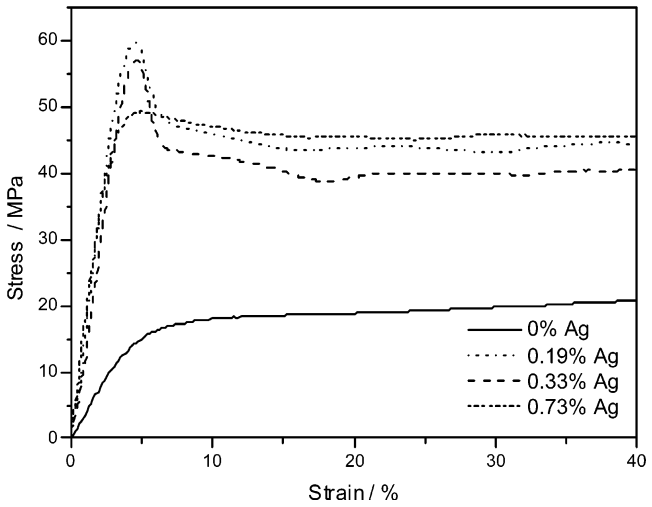

Figure 7. Stress−strain behavior of the pure PVA and PVA−Ag nanocomposite films with varying Ag wt % contents.

of the polystyrene−CdS nanocomposite.[20] Because of the formation of chemical bonds between the polystyrene chains and sulfur, originating from the surface of the 50-Å CdS nanoparticles, the thermal stability of the nanocomposite was improved by about 100 °C. On the other hand, up to 10 wt %, PVA−MMT nanocomposites showed almost the same thermal stability as that of pure PVA,[27] while the thermal stability of the PVA filled with magnetite nanoparticles was reduced by 28 °C.[26]

Mechanical and Viscoelastic Characterization of the PVA−Ag Nanocomposites. Figure 7 depicts typical stress−strain curves of pure PVA and nanocomposites with different Ag loadings. A change in the stress−strain behavior after introduction of nanoparticles in the matrix can be seen. Contrary to the pure matrix, where stress monotonically increases after initial elastic deformation, the nanocomposite films exhibit a clearly distinguished yield point. The nanoparticles, obviously, affect the structural rearrangements during the post-elastic deformation to induce semicrystalline-like mechanical behavior. Sharaf et al.[33] have observed a similar trend with a micro-sized $FeSO_4$ filler, but at higher filler loadings (>10 wt %). In Figure 8 Young's modulus, and stress and strain at break, are plotted vs silver content. The initial modulus of the pure PVA is about 380 MPa, which is higher than the reported bulk value of 68 MPa.[27] The reason for the observed discrepancy is a different measuring procedure. We were interested in the mechanical properties of the as-prepared films, and they were not preconditioned in 50% humidity as has been done in the above-mentioned investigation on PVA−MMT nanocomposites. Nevertheless, despite different experimental procedures, the effects of the nanofiller on the mechanical properties of PVA in both studies are comparable. Depending on the filler content, nanocomposite films show up to 4× higher modulus than the matrix. The high bulk-to-surface ratio of the nanoparticles (short interparticle distance), as well as attachment of PVA chains to their surface, are the reasons for this behavior. Because of the attachment of polymer segments, the transfer of mechanical energy from the matrix to the high-modulus

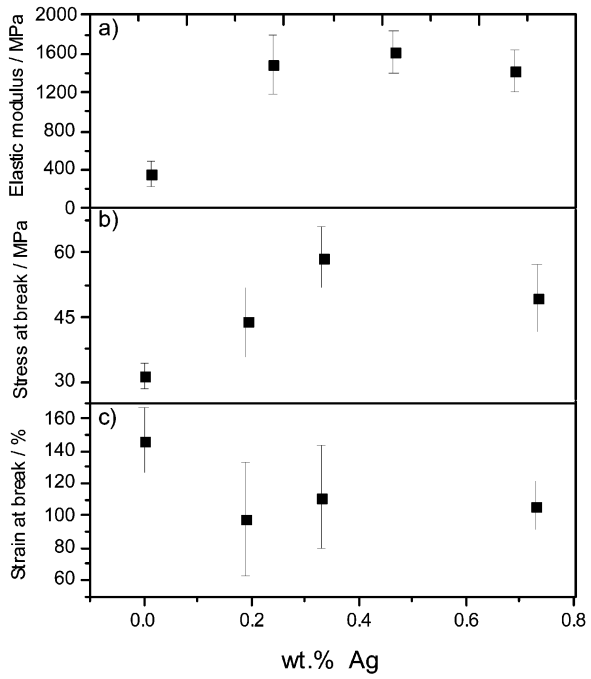

Figure 8. (a) Young's elastic modulus, (b) stress at break, and (c) strain at break as a function of Ag content. (Deformation rate 50 mm min^{-1})

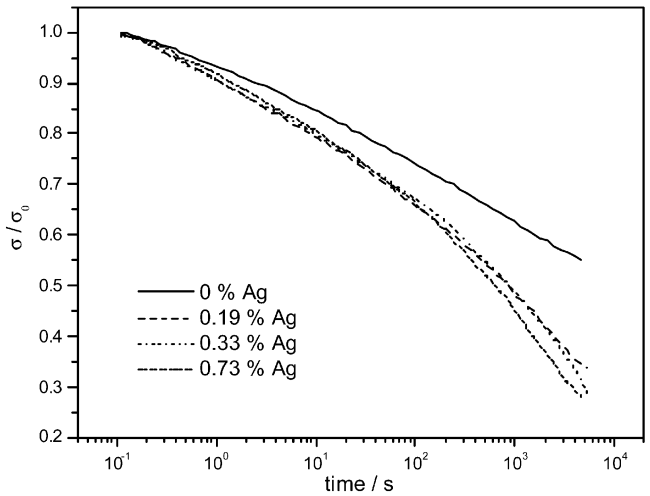

Figure 9. Stress relaxation of neat PVA and PVA−Ag nanocomposite films with varying Ag wt % contents. (Constant strain 2%, deformation rate 50 mm min^{-1}).

filler will be significantly enhanced, i.e., the modulus of the material as a whole increases. On the other hand, because the concentration of the nanoparticles is low, increasing of the modulus cannot be interpreted solely with a high filler modulus. It is rather that the chains in the matrix−nanoparticle interfacial regions are so highly immobilized that they exhibit enhanced stiffness compared to the rest of the matrix. In fact, one should talk about effective size of the filler particle, which includes these interfacial regions. Because the distance between the nanoparticles is small (about 100 nm from TEM measurements), inclusion of these interfacial regions into the effective particle size means that almost the whole matrix is affected. As a result, instead of a continuous increase, Young's modulus of the nanocomposite jumps up to a 2 or 3× higher value at quite low nanoparticle concentrations (Figure 8a). Also, if one

(33) Sharaf, F.; Mansour, S. A.; El-Lawindy, A. M. Y. *Polym. Degrad. Stab.* **1999**, *66*, 173.

treats domains with enhanced stiffness as "crystals" in the softer matrix, this can explain semicrystalline-like deformation behavior of the nanocomposite observed in Figure 7. Another effect, which is in line with the former conclusions, is the strong influence of nanoparticles on the material strength. It can be seen in Figure 8b that the stress at break of the nanocomposite film with 0.33 wt % of silver nanoparticles is almost 100% higher than that of the matrix. Finally, the strain at break slightly decreases with increasing nanoparticle content (Figure 8c). This result is in agreement with previous investigations on PVA−MMT nanocomposites,[27] where changes in strain at break were within a few percent even at high MMT loadings.

Figure 9 shows stress relaxation of PVA and PVA−Ag nanocomposites, normalized with respect to initial stress. It can be seen that normalized residual stress (after 90 min) decreases with an increase in nanoparticle content. This means that nanocomposite films show reduced stability on prolonged loading. Similar results were obtained in our previous study on polystyrene−hematite nanocomposites.[22] Although nanoparticles reinforce the matrix to a high extent, it seems as if they influence the viscoelastic properties to favor the cold flow. It is possible that this is a consequence of the debonding process that takes place during the loading of samples prior to stress relaxation.[22] Because of the debonding process, the average free volume increases, which allows easier structural rearrangements of polymer chains during the stress relaxation. Because of this, stress decay will be more pronounced and the normalized residual stress will decrease (Figure 9).

Conclusions

The incorporation of an Ag-nanofiller into the PVA matrix induced significant changes in the thermal and mechanical properties of the PVA, even when the content of the inorganic phase was extremely low (<1 wt %). For example, the glass transition was shifted toward higher temperatures by 20 °C, and the thermal stability was improved by about 40 °C in the case of the nanocomposite containing 0.73 wt % of Ag. Nanocomposite films showed deformation behavior characteristic of semicrystalline-type materials with a clearly distinguished yield point. No yield point was observed in deformation of the pure PVA matrix. These changes in the thermal and mechanical behavior of the PVA, in the presence of the Ag-nanofiller, were discussed in terms of polymer chains attached to the surface of Ag nanoparticles, and this is supported by FTIR data.

CM034505A